crystals

Experimental Sensing and DFT Mechanism of Zn(II) Complex for Highly Sensitive and Selective Detection of Acetone

Mohd. Muddassir [1,*], Mohammad Usman [2], Abdullah Alarifi [1], Mohd. Afzal [1], Khulud Abdullah Alshali [1], Abeer Beagan [1], Abhinav Kumar [3], Naaser A. Y. Abduhd [1] and Musheer Ahmad [4,*]

[1] Department of Chemistry, College of Science, King Saud University, Riyadh 11451, KSA; arifi@ksu.edu.sa (A.A.); Afzalanalytical@gmail.com (M.A.); 437202938@student.ksu.edu.sa (K.A.A.); abeagan@ksu.edu.sa (A.B.); 439106262@ksu.edu.sa (N.A.Y.A.)
[2] Department of Chemistry, IIT Kanpur, Uttar Pradesh 208016, India; mohammadusman148@gmail.com
[3] Department of Chemistry, Faculty of Science, University of Lucknow, 226 007, India; abhinavmarshal@gmail.com; abhinavmarshal@gmail.com
[4] Department of Applied Chemistry, Aligarh Muslim University, Aligarh 202002, India
* Correspondence: mmohammadarshad@ksu.edu.sa (M.M.) amusheer4@gmail.com (M.A.)

Crystal structure determination

Single crystals of Zn complex were coated with a trace of Fomblin oil and quickly transferred to the goniometer head of a Bruker Quest diffractometer with a fixed chi angle, a sealed tube fine focus X–ray tube, single crystal curved graphite incident beam monochromator, a Photon100 CMOS area detector and an Oxford Cryosystems low-temperature device. Examination and data collection were performed with Mo Kα radiation (λ = 0.71073 Å) at 150 K.

Data were collected, reflections were indexed and processed, and the files scaled and corrected for absorption using APEX3[1]. The space groups were assigned, and the structures were solved by direct methods using XPREP within the SHELXTL suite of programs [2,3] and refined by full–matrix least squares against F^2 with all reflections using Shelxl2018 [4,5] using the graphical interface Shelxle[6]. H atoms attached to carbon and nitrogen atoms as well as hydroxyl hydrogens were positioned geometrically and constrained to ride on their parent atoms. C–H bond distances were constrained to 0.95 Å for aromatic and alkene C-H moieties. N–H bond distances were constrained to 0.88 Å for planar (sp^2 hybridized) N-H groups. Figures were drawn using ORTEP–3.3 [7] and MERCURY–4.1.0 [8].

Computational methodology

The full geometry optimizations have been carried out at DFT level of theory using the B3LYP functional [9–11] with the help of the Gaussian−09 program package [12]. The calculations were performed using 6−31G* basis sets[13,14] for C, H, N, O, Cl atoms and def2-TZVP basis set for Zn atom. All the DFT calculations were performed with counter ions by employing the polarizable continuum model, CPCM (DMSO as solvent) [15–17]. No symmetry restrictions have been applied during geometry optimization. The Hessian matrix was calculated analytically for the optimized structures in order to prove the location of correct minima (no imaginary frequencies). The Cartesian atomic coordinates of the calculated optimized structures in DMSO are also provided below.

Zn-complex

1	30	−1.495821000	−0.196993000	0.444160000
2	8	−2.227674000	0.981163000	2.045308000
3	1	−3.188971000	0.891123000	2.159155000
4	1	−2.064962000	1.951545000	1.888098000
5	7	0.425101000	−0.215333000	1.378902000
6	7	−0.171200000	−0.250000000	−1.230480000

7	7	−3.379396000	−0.130428000	−0.590478000
8	7	−2.228871000	−2.164759000	0.726952000
9	6	−3.298658000	−4.715957000	0.892405000
10	1	−3.723808000	−5.712595000	0.950449000
11	6	3.005732000	−0.286110000	2.386218000
12	1	4.023022000	−0.314416000	2.762817000
13	6	−0.553641000	−0.266974000	−2.515545000
14	1	−1.619856000	−0.193814000	−2.699430000
15	6	2.786282000	−0.343339000	1.010846000
16	1	3.632441000	−0.419779000	0.340000000
17	6	−3.975111000	−3.710669000	0.203556000
18	1	−4.921123000	−3.930462000	−0.274169000
19	6	−3.416869000	−2.430985000	0.136565000
20	6	−4.071104000	−1.292703000	−0.566746000
21	6	1.141972000	−0.337586000	−0.918842000
22	6	−1.578543000	−3.132927000	1.388916000
23	1	−0.632236000	−2.852883000	1.839111000
24	6	1.710954000	−0.465354000	−3.253777000
25	1	2.453333000	−0.550835000	−4.040882000
26	6	−5.874118000	−0.265966000	−1.789828000
27	1	−6.851739000	−0.327432000	−2.256782000
28	6	1.474679000	−0.302569000	0.531089000
29	6	0.355368000	−0.371993000	−3.563937000
30	1	0.003098000	−0.379912000	−4.589096000
31	6	0.638523000	−0.154829000	2.702029000
32	1	−0.247563000	−0.068456000	3.321011000
33	6	2.113295000	−0.448667000	−1.919169000
34	1	3.165576000	−0.525178000	−1.670425000
35	6	1.917696000	−0.188281000	3.251805000
36	1	2.047156000	−0.136627000	4.326937000
37	6	−5.331062000	−1.387238000	−1.164402000
38	1	−5.890891000	−2.313443000	−1.142321000
39	6	−5.153525000	0.926551000	−1.802465000
40	1	−5.543456000	1.821102000	−2.274585000
41	6	−3.904922000	0.952196000	−1.185718000
42	1	−3.299480000	1.853306000	−1.155864000
43	6	−2.078276000	−4.427099000	1.499888000
44	1	−1.521128000	−5.179705000	2.045753000
45	17	−1.039830000	4.029542000	0.398788000
46	8	−1.862114000	3.636101000	1.613646000
47	8	0.357529000	3.542544000	0.578910000
48	8	−1.066215000	5.510640000	0.278227000
49	8	−1.644370000	3.401737000	−0.818009000

50	17	6.540888000	−0.560175000	−0.471796000
51	8	7.099477000	0.559377000	−1.287941000
52	8	7.568229000	−1.632115000	−0.306143000
53	8	5.340479000	−1.136617000	−1.170579000
54	8	6.130378000	−0.044622000	0.873452000

Zn-complex + acetone

1	30	−1.734924000	−0.158995000	0.401872000
2	8	−3.007393000	0.736617000	1.834120000
3	1	−3.914048000	0.389412000	1.783234000
4	1	−3.088677000	1.717302000	1.679958000
5	7	−0.065444000	0.417277000	1.590668000
6	7	−0.231553000	0.153065000	−1.065495000
7	7	−3.422574000	−0.606130000	−0.865139000
8	7	−1.975100000	−2.239813000	0.697305000
9	6	−2.421762000	−4.965162000	0.931156000
10	1	−2.603486000	−6.031562000	1.016979000
11	6	2.229030000	1.166765000	2.946972000
12	1	3.132327000	1.460352000	3.472282000
13	6	−0.391273000	−0.022207000	−2.385240000
14	1	−1.386299000	−0.300538000	−2.714904000
15	6	2.243665000	1.042570000	1.558492000
16	1	3.157621000	1.234984000	1.008258000
17	6	−3.234422000	−4.185506000	0.109255000
18	1	−4.040842000	−4.650025000	−0.443621000
19	6	−2.990462000	−2.813280000	0.008927000
20	6	−3.806224000	−1.902817000	−0.842345000
21	6	0.980443000	0.500330000	−0.575575000
22	6	−1.187120000	−2.991844000	1.479691000
23	1	−0.371501000	−2.479389000	1.975529000
24	6	1.905338000	0.496239000	−2.796958000
25	1	2.752709000	0.625143000	−3.462411000
26	6	−5.623593000	−1.409414000	−2.344426000
27	1	−6.483907000	−1.732438000	−2.921582000
28	6	1.069700000	0.661544000	0.900956000
29	6	0.652554000	0.138584000	−3.291897000
30	1	0.479700000	−0.015420000	−4.350959000
31	6	−0.078890000	0.542459000	2.926323000
32	1	−1.028371000	0.345474000	3.411359000
33	6	2.073916000	0.683447000	−1.426114000
34	1	3.047724000	0.956506000	−1.039658000
35	6	1.051052000	0.914271000	3.648678000
36	1	1.000981000	1.003142000	4.727947000

37	6	−4.913398000	−2.333188000	−1.579474000
38	1	−5.227293000	−3.368860000	−1.560776000
39	6	−5.220723000	−0.075479000	−2.354500000
40	1	−5.749580000	0.673418000	−2.933006000
41	6	−4.111257000	0.286305000	−1.594267000
42	1	−3.755370000	1.311376000	−1.552916000
43	6	−1.377755000	−4.363050000	1.629195000
44	1	−0.718775000	−4.934797000	2.272422000
45	17	−2.459442000	4.017534000	0.291935000
46	8	−3.316678000	3.397337000	1.381247000
47	8	−1.042443000	4.057606000	0.751634000
48	8	−2.963540000	5.390620000	0.027534000
49	8	−2.568525000	3.180866000	−0.944972000
50	17	6.078765000	0.662643000	−0.814289000
51	8	7.240300000	1.412286000	−1.377212000
52	8	6.559827000	−0.336886000	0.190657000
53	8	5.353677000	−0.044718000	−1.919576000
54	8	5.142857000	1.631198000	−0.146237000
55	6	3.040198000	−2.747079000	0.469608000
56	8	1.858406000	−2.524678000	0.698946000
57	6	4.089809000	−2.669934000	1.557898000
58	1	4.871822000	−1.954251000	1.274445000
59	1	3.633959000	−2.369837000	2.504008000
60	1	4.577990000	−3.645185000	1.678080000
61	6	3.529412000	−3.088398000	−0.921961000
62	1	4.158873000	−3.985682000	−0.903928000
63	1	2.682996000	−3.239996000	−1.595639000
64	1	4.152014000	−2.265987000	−1.298128000

Table 1. Crystallographic data of {[Zn(bipy)$_2$(H$_2$O)](ClO$_4$)$_2$} (**1**).

CCDC No.	CCDC 766185
Color	Colorless
Molecular formula	$C_{20}H_{18}N_4OZn.2(ClO_4)$
Molecular weight (g/mol)	594.65
Crystal system	P21/c
Space group	Monoclinic
a (Å)	8.988 (3)
b (Å)	12.812 (4)
c (Å)	19.921 (5)
U (Å^3)	2214.8 (12)
β = (°)	105.095 (12)

DX (Mg m−3)	1.783
Z	4
F (000)	1208
Crystal size/mm	0.30 × 0.25 × 0.20
μ(mm^{-1})	1.41
θ (°)	2.4–27.5
Index ranges	−10 < h < 10; −15 < k < 14; −15 < l < 23
No. of reflections collected	1115
No. of independent reflections (Rint)	3907 (0.055)
No. of observed [I >2σ(I)] reflections	3218
No. of data/restraints/ parameters	3907/0/325
R[F2 > 2σ(F2)]	0.050
wR(F2)	0.129
Δρmax and Δρmin (e $Å^{-3}$)	0.77 and −0.81

Table 2. Selected bond lengths [Å] and bond angles [°] of {[Zn(bipy)$_2$(H_2O)](ClO_4)$_2$} (**1**).

Zn—O1	2.028 (3)	Zn—N2	2.061 (3)
Zn—N4	2.070 (3)	Zn—N1	2.091 (3)
Zn—N3	2.104 (3)		
O1—Zn—N2	118.99 (11)	O1—Zn—N4	121.81 (12)
N2—Zn—N4	119.18 (12)	O1—Zn—N189.67 (11)	
N2—Zn—N1	79.03 (13)	N4—Zn—N1	102.44 (13)
O1—Zn—N3	90.58 (10)	N2—Zn—N3	99.86 (12)
N4—Zn—N3	78.39 (12)	N1—Zn—N3	178.83 (13)
Zn—O1—H1A	121.2	Zn—O1—H1B	107.0
C12—N1—Zn	115.0 (3)	C3—N2—C8	119.0 (3)
C3—N2—Zn	126.1 (2)	C8—N2—Zn	114.9 (2)
C7—N3—C19	118.4 (3)	C7—N3—Zn	114.7 (2)
C19—N3—Zn	126.3 (3)	C9—N4—C6	118.8 (3)
C9—N4—Zn	125.7 (3)	C6—N4—Zn	115.4 (2)

Table 3. The origin of the transitions from IR, NMR, UV-Vis and TGA and its description.

IR(KBr, cm^{-1})	**NMR (^{1}H: DMSO–*d_6*, 400 MHz) δ (ppm) ^{13}C: (DMSO–*d_6*, 100 MHz)**	**UV-Vis UV–Vis (DMSO, nm):**	**TGA (°C) (25−800 °C)**
3481(OH, H_2O); 3101 (CH, aromatic); 1442 (CH, aromatic); 1601, 1576, 1493 (bipyridyl N); 1100 (ClO_4); 413 (Zn–O); 415 (Zn–N)	^{1}H NMR; 7.8–8.7 (Ar–H); 3.4 (H_2O); 1.0 (trace amount of lattice Ethanol). ^{13}C NMR; 123–149 (Ar–C)	209 (π–π*) 295 (LMCT)	75–160 (Removal of traces of ethanol) 210–350 (Removal of coordinated water molecules)

					320–360 (Removal of both the perchlorate anions) 365–600 (Decomposition of the bipyridyl group) 610–800 (Formation of Zinc oxide)

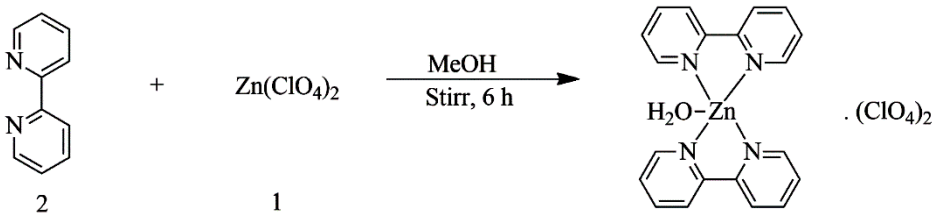

Scheme S1. Synthetic scheme of complex {[Zn(bipy)$_2$(H$_2$O)](ClO$_4$)$_2$} (**1**).

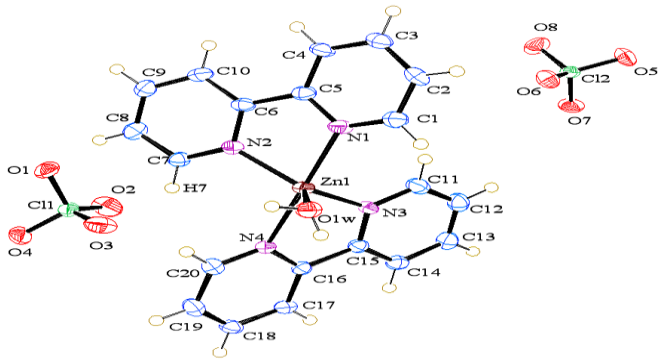

Figure S1. Ellipsoidal presentation of the molecular structure of complex {[Zn(bipy)$_2$(H$_2$O)](ClO$_4$)$_2$} (**1**) with 30% probability factor.

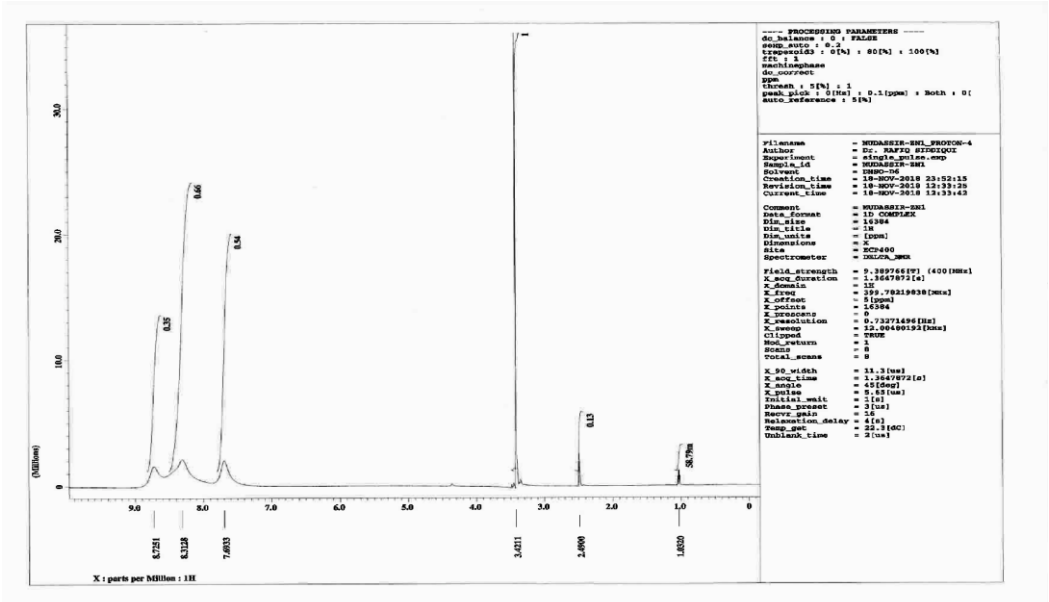

Figure 2. The ^{1}H NMR spectrum of complex {[Zn(bipy)$_2$(H$_2$O)](ClO$_4$)$_2$} (**1**) in DMSO-d6 at room temperature.

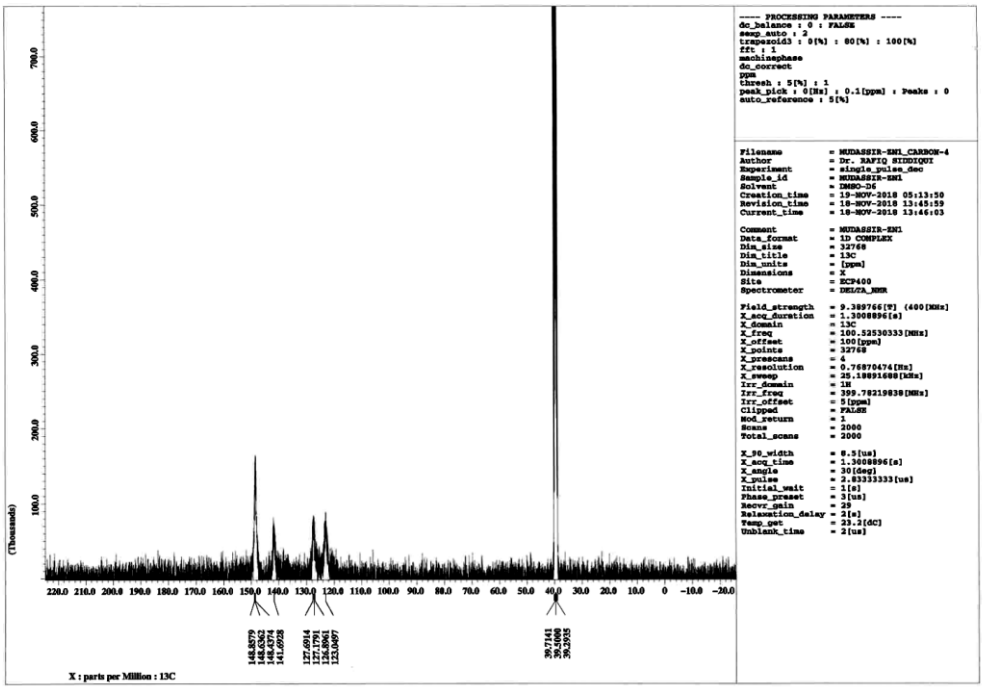

Figure S3. The ^{13}C NMR spectrum of complex {[Zn(bipy)$_2$(H$_2$O)](ClO$_4$)$_2$} (**1**) in DMSO-d6 at room temperature.

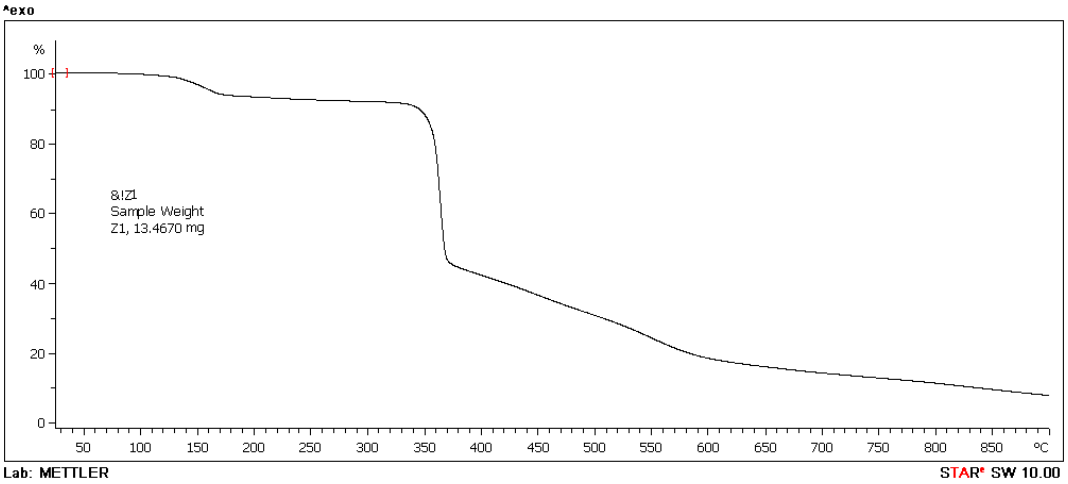

Figure S4. Thermogravimetric analysis of complex {[Zn(bipy)$_2$(H$_2$O)](ClO$_4$)$_2$} (**1**).

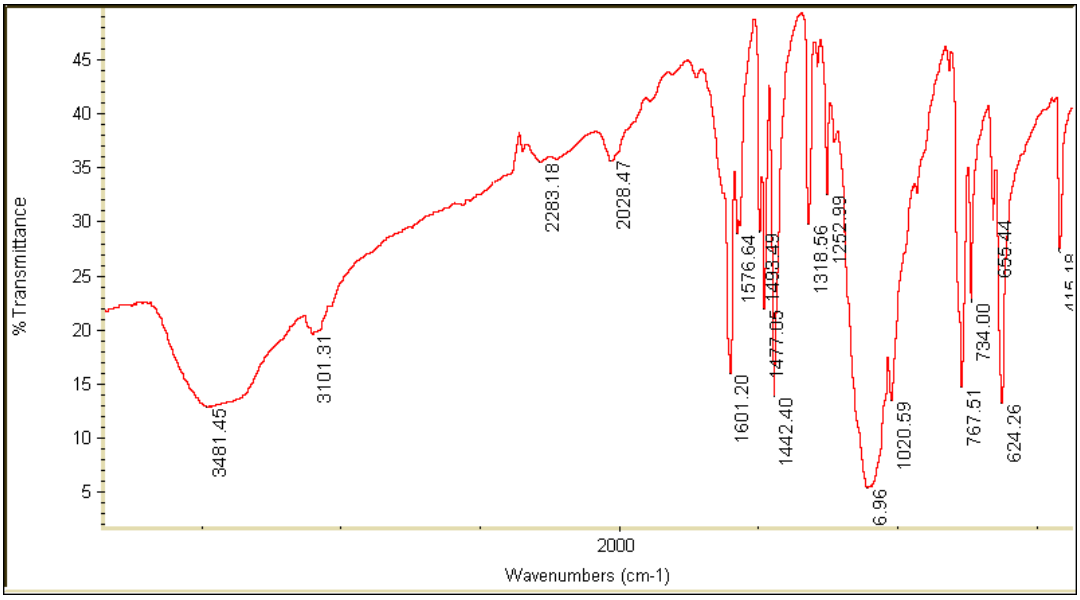

Figure S5. IR spectrum of complex {[Zn(bipy)$_2$(H$_2$O)](ClO$_4$)$_2$} (**1**).

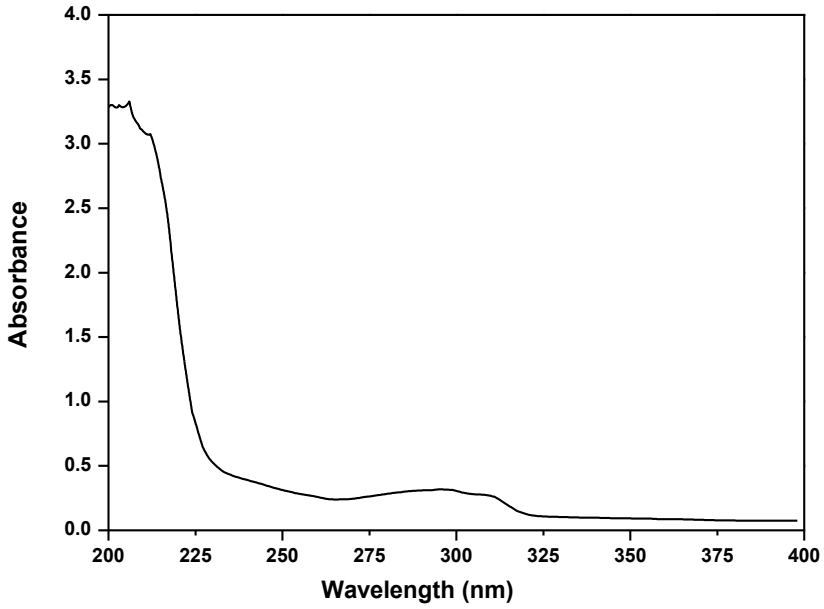

Figure S6. UV-Vis Spectrum of complex {[Zn(bipy)$_2$(H$_2$O)](ClO$_4$)$_2$} (**1**).

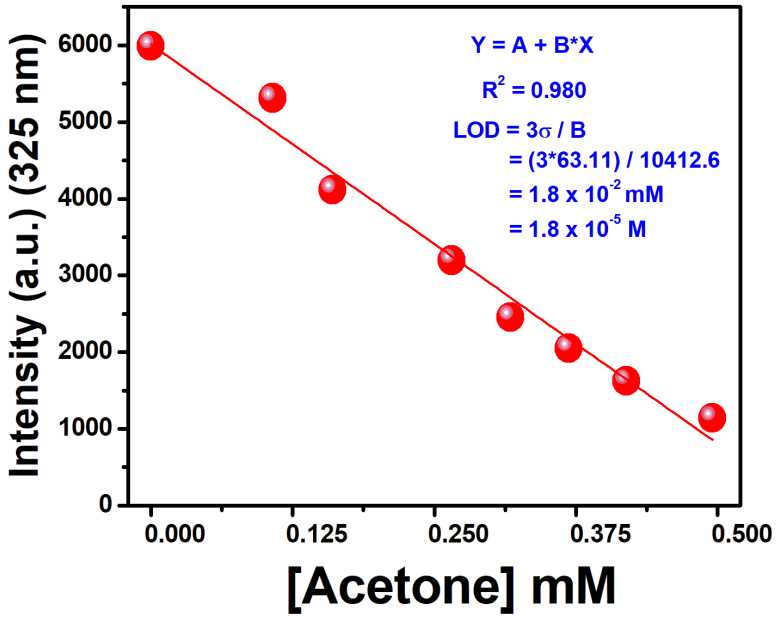

Figure S7. Normalized response of fluorescence signal of complex {[Zn(bipy)$_2$(H$_2$O)](ClO$_4$)$_2$} (**1**) in the presence of increasing amount of acetone (0 to 1.05 mM) predissolved in DMSO. (λ_{ex}= 295nm; λ_{em}= 325nm).

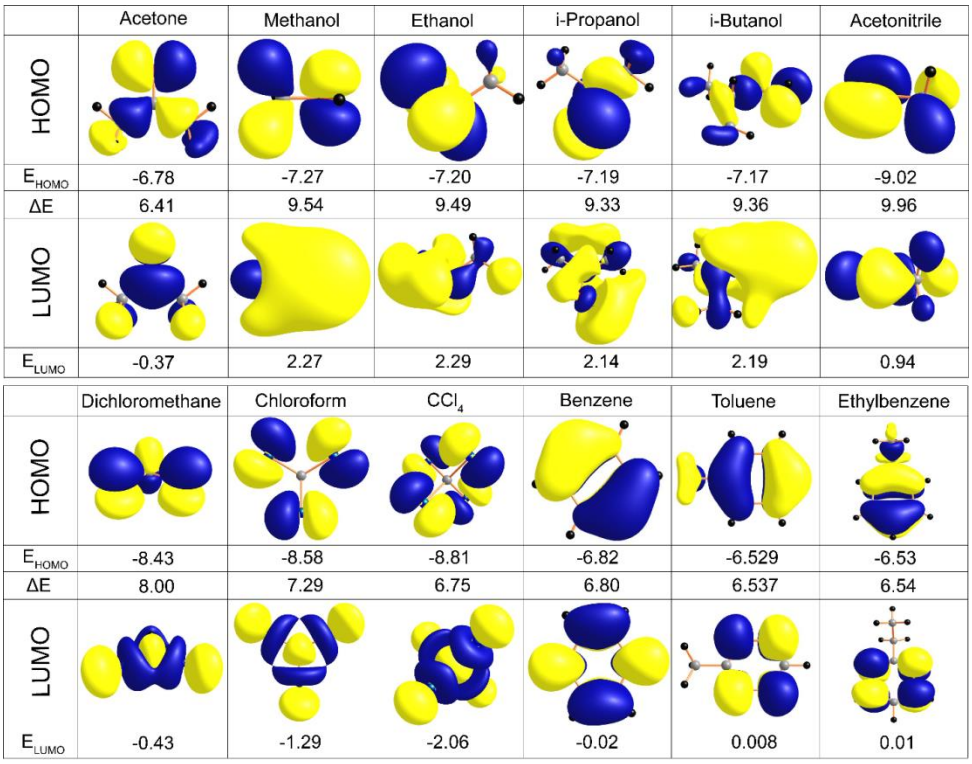

Figure S8. Frontier molecular orbital of various molecules used in sensing studies.

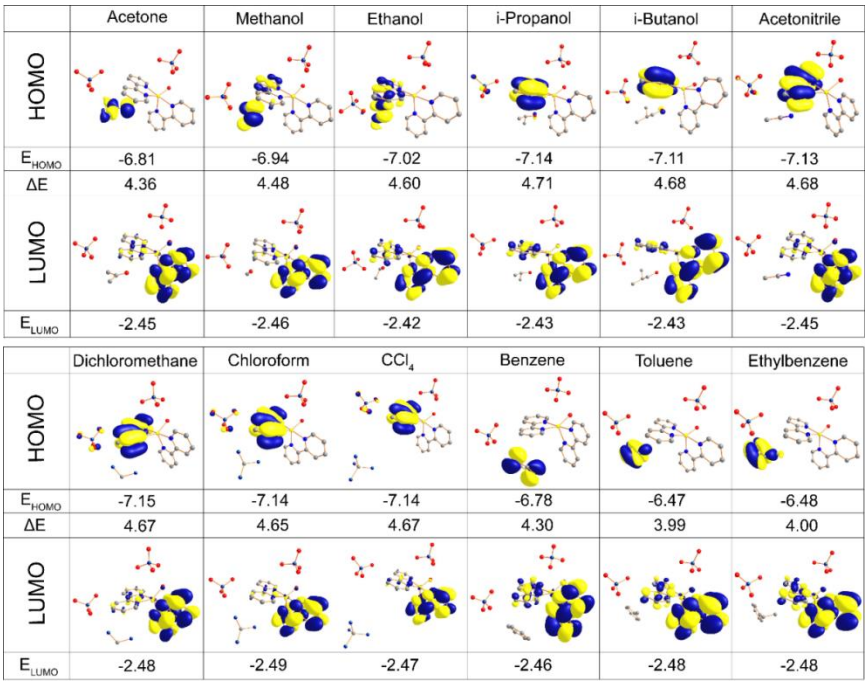

Figure S9. Frontier molecular orbital of the aggregate of complex {[Zn(bipy)$_2$(H$_2$O)](ClO$_4$)$_2$} (**1**) with the various used solvents.

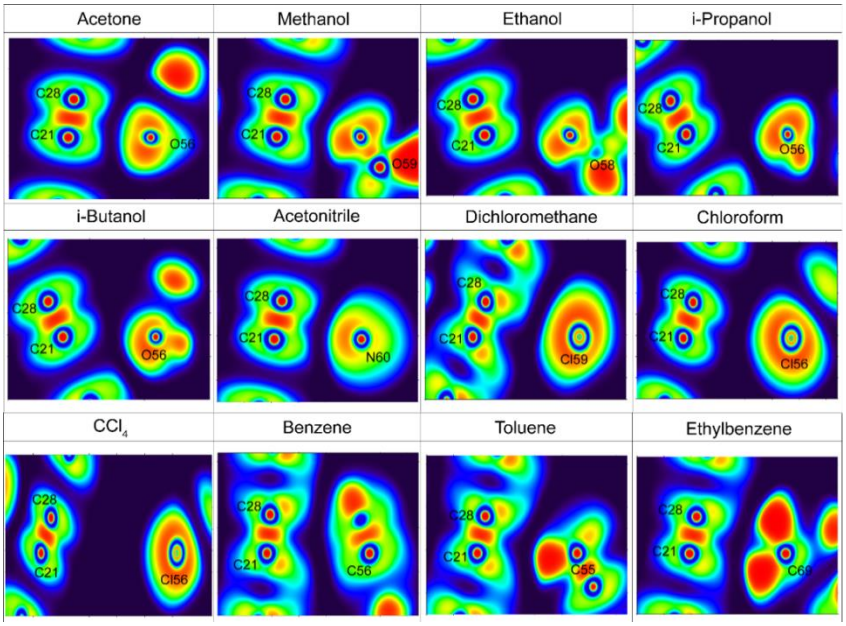

Figure S10. Electron localization function (ELF) map of the aggregate of complex {[Zn(bipy)$_2$(H$_2$O)](ClO$_4$)$_2$} (**1**) in different solvents.

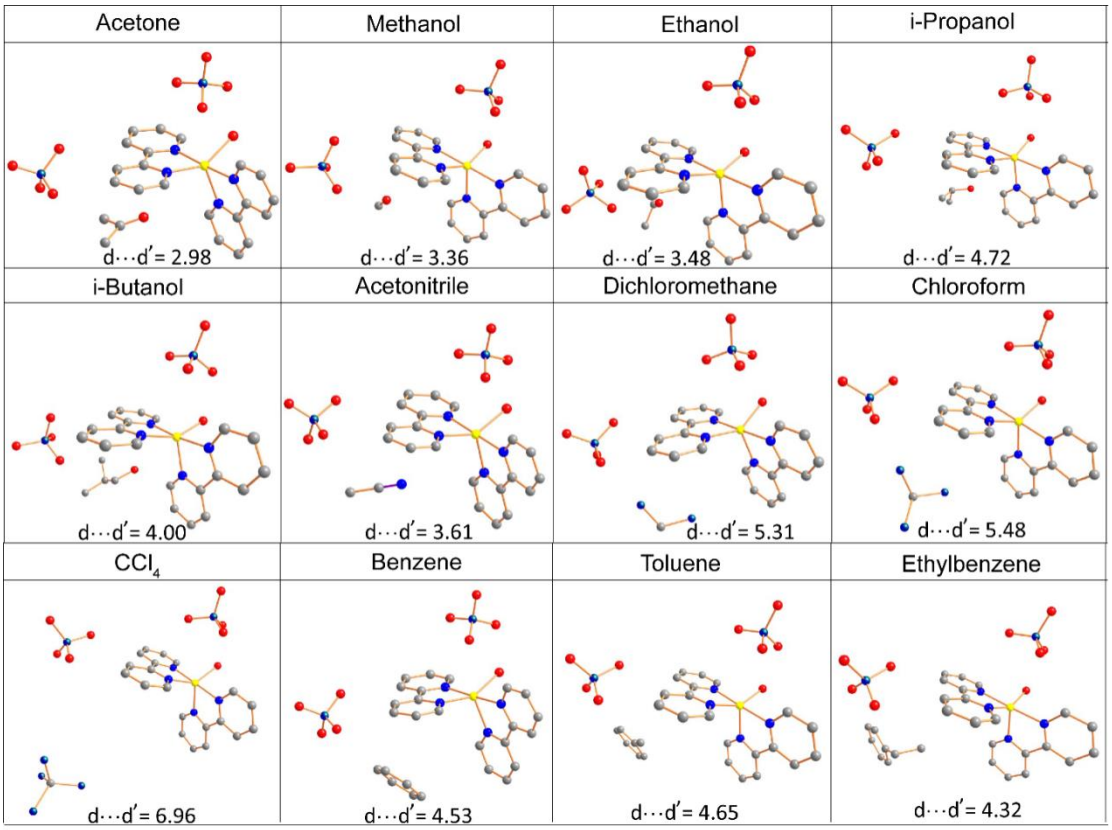

Figure S11. B3LYP/DFT optimized structures of the aggregate of complex {[Zn(bipy)$_2$(H$_2$O)](ClO$_4$)$_2$} (**1**) in presence of various organic solvents for sensing. The d···d′ distance in angstrom represents the nearest distance between the carbon atoms of bipyridyl moiety of Zn(II)-complex and different solvents.

References

[1] Bruker (2016). Apex3 v2016.9−0, Saint V8.34A, SAINT V8.37A, Bruker AXS Inc.: Madison (WI), USA, 2013/2014, (2016).

[2] SHELXTL suite of programs, Version 6.14, 2000−2003, Bruker Advanced X-ray Solutions, Bruker AXS Inc., Madison, Wisconsin: USA, (n.d.).

[3] G.M. Sheldrick, A short history of SHELX., Acta Crystallogr. A. 64 (2008) 112–22. doi:10.1107/S0108767307043930.

[4] Sheldrick George M. University of Göttingen, Germany., (2018).

[5] G.M. Sheldrick, Crystal structure refinement with SHELXL., Acta Crystallogr. Sect. C, Struct. Chem. 71 (2015) 3–8. doi:10.1107/S2053229614024218.

[6] C.B. Hübschle, G.M. Sheldrick, B. Dittrich, ShelXle: A Qt graphical user interface for SHELXL, J. Appl. Crystallogr. 44 (2011) 1281–1284. doi:10.1107/S0021889811043202.

[7] L.J. Farrugia, ORTEP−3 for windows - A version of ORTEP-III with a graphical user interface (GUI), J. Appl. Crystallogr. 30 (1997) 565. doi:10.1107/S0021889897003117.

[8] C.F. Macrae, P.R. Edgington, P. McCabe, E. Pidcock, G.P. Shields, R. Taylor, M. Towler, J. van de Streek, Mercury : visualization and analysis of crystal structures , J. Appl. Crystallogr. 39 (2006) 453–457. doi:10.1107/s002188980600731x.

[9] A.D. Becke, Density-functional thermochemistry. III. The role of exact exchange, J. Chem. Phys. 98 (1993) 5648–5652. doi:10.1063/1.464913.

[10] C. Lee, W. Yang, R.G. Parr, Development of the Colle-Salvetti correlation-energy formula into a functional of the electron density, Phys. Rev. B. 37 (1988) 785–789. doi:10.1103/PhysRevB.37.785.

[11] P.J. Stephens, F.J. Devlin, C.F. Chabalowski, M.J. Frisch, Ab Initio Calculation of Vibrational Absorption and Circular Dichroism Spectra Using Density Functional Force Fields, J. Phys. Chem. 98 (1994) 11623–

11627. doi:10.1021/j100096a001.

[12] M.J.. Frisch, G.W.. Trucks, H.B.. Schlegel, G.E.. Scuseria, M.A.. Robb, J.R.. Cheeseman, G.. Scalmani, V.. Barone, B.. Mennucci, G.A.. Petersson, H.. Nakatsuji, M.. Caricato, X.. Li, H.P.. Hratchian, A.F.. Izmaylov, J.. Bloino, G.. Zheng, J.L.. Sonnenberg, M.. Hada, M.. Ehara, K.. Toyota, R.. Fukuda, J.. Hasegawa, M.. Ishida, T.. Nakajima, Y.. Honda, O.. Kitao, H.. Nakai, T.. Vreven, J.. Montgomery, J. A., J.E.. Peralta, F.. Ogliaro, M.. Bearpark, J.J.. Heyd, E.. Brothers, K.N.. Kudin, V.N.. Staroverov, R.. Kobayashi, J.. Normand, K.. Raghavachari, A.. Rendell, J.C.. Burant, S.S.. Iyengar, J.. Tomasi, M.. Cossi, N.. Rega, J.M.. Millam, M.. Klene, J.E.. Knox, J.B.. Cross, V.. Bakken, C.. Adamo, J.. Jaramillo, R.. Gomperts, R.E.. Stratmann, O.. Yazyev, A.J.. Austin, R.. Cammi, C.. Pomelli, J.W.. Ochterski, R.L.. Martin, K.. Morokuma, V.G.. Zakrzewski, G.A.. Voth, P.. Salvador, J.J.. Dannenberg, S.. Dapprich, A.D.. Daniels, Ö.. Farkas, J.B.. Foresman, J.V.. Ortiz, J.. Cioslowski, D.J. Fox, Gaussian 09 Citation | Gaussian.com, Gaussian, Inc., Wallingford CT,. (2009). http://gaussian.com/g09citation/ (accessed November 11, 2019).

[13] P.J. Hay, W.R. Wadt, Ab initio effective core potentials for molecular calculations. Potentials for the transition metal atoms Sc to Hg, J. Chem. Phys. 82 (1985) 270–283. doi:10.1063/1.448799.

[14] W.R. Wadt, P.J. Hay, Ab initio effective core potentials for molecular calculations. Potentials for main group elements Na to Bi, J. Chem. Phys. 82 (1985) 284–298. doi:10.1063/1.448800.

[15] V. Barone, M. Cossi, Quantum Calculation of Molecular Energies and Energy Gradients in Solution by a Conductor Solvent Model, J. Phys. Chem. A. 102 (1998) 1995–2001. doi:10.1021/jp9716997.

[16] M. Cossi, V. Barone, Time-dependent density functional theory for molecules in liquid solutions, J. Chem. Phys. 115 (2001) 4708–4717. doi:10.1063/1.1394921.

[17] M. Cossi, N. Rega, G. Scalmani, V. Barone, Energies, structures, and electronic properties of molecules in solution with the C-PCM solvation model, J. Comput. Chem. 24 (2003) 669–681. doi:10.1002/jcc.10189.